The antiferromagnet/superconductor proximity effect in Cr/V/Cr trilayers

2002 J. Phys.: Condens. Matter 14 8687

(http://iopscience.iop.org/0953-8984/14/37/305)

INSTITUTE OF PHYSICS PUBLISHING JOURNAL OF PHYSICS: CONDENSED MATTER

J. Phys.: Condens. Matter **14** (2002) 8687–8696 PII: S0953-8984(02)36920-0

The antiferromagnet/superconductor proximity effect in Cr/V/Cr trilayers

M Hübener[1], D Tikhonov[2], I A Garifullin[2], K Westerholt[1] and H Zabel[1]

[1] Fakultät für Physik und Astronomie, Lehrstuhl für Experimentalphysik/Festkörperphysik, Ruhr-Universität Bochum, D-44780 Bochum, Germany
[2] Kazan Physicotechnical Institute of Russian Academy of Sciences, 420029 Kazan, Russia

E-mail: hartmut.zabel@ruhr-uni-bochum.de

Received 13 May 2002, in final form 13 August 2002
Published 5 September 2002
Online at stacks.iop.org/JPhysCM/14/8687

Abstract

We have studied the superconducting properties of (110) textured Cr/V/Cr trilayers grown on $Al_2O_3(1\bar{1}20)$, representing an antiferromagnet/superconductor (AF/SC) proximity system. We have prepared several series of samples with either d_V, the thickness of the V layer, or d_{Cr}, the thickness of the Cr layer being constant, while varying the other thickness. We find an overall good agreement with the classical Werthamer theory of the AF/SC proximity effect, with one noticeable exception. When plotting the superconducting transition temperature as a function of the thickness d_{Cr}, we find an anomalous drop of $T_c(d_{Cr})$ at $d_{Cr} \approx 6$ nm with a sudden quenching of the superconductivity for layer thicknesses $d_{Cr} \geqslant 6$ nm. We argue that this drop of T_c might be correlated with the onset of an incommensurate spin density wave state in the Cr film.

(Some figures in this article are in colour only in the electronic version)

1. Introduction

The proximity effect at the interface of a superconductor (SC) and a non-superconducting metal, which can be a normal metal (NM), a ferromagnet (FM) or an antiferromagnet (AF), is a classical subject in superconductivity. The theoretical description of the proximity effect, which principally still holds today, dates back to the early 1960s [1]. Only for the special case of the SC/FM proximity effect has there been an essential further development in recent years, initiated by new experimental findings, such as π-wave superconductivity in SC/FM/SC trilayers [2, 3] and oscillating superconducting transition temperatures in FM/SC/FM sandwich structures with varying thickness of the FM layers, including re-entrant superconductivity with increasing FM layer thickness [4, 5], which motivated new theoretical work [6]. For a recent overview of the FM/SC proximity effect we refer the reader to [7]. In the classical work by Werthamer [1], the proximity effect for a superconducting layer and an AF (the SC/AF proximity effect) is treated like the SC/NM proximity effect, since within the superconducting

correlation length ξ_s the magnetic moments of the AF are compensated and the magnetic order is irrelevant to the superconductivity. The only additional factor, which must be considered unlike for normal metals, is the magnetic defects, such as uncompensated spins in the AF or at the interfaces. These defects induce magnetic pair-breaking scattering which can be included theoretically by introducing a finite magnetic scattering time. The experiments on SC/AF systems, such as Pb/Cr and Nb/Cr, have been interpreted following these lines of argumentation [8, 9]. The V/Cr system was more recently studied by Davis *et al* [10]. The authors found a drop of the superconducting transition temperature T_c with increasing Cr thickness and a curious increase of T_c at a Cr thickness of about 5 nm, which could not be explained.

The magnetic ground state in bulk Cr is not of conventional AF type, but it is an incommensurate spin density wave (SDW) state with a period of about 6 nm at low temperatures and propagating along the [100] and equivalent directions [11]. In bulk Cr the incommensurate SDW develops below the Néel temperature of $T_N = 311$ K. The SDW magnetism of Cr has attracted much interest in the past since its first discovery [12–14]. More recently, attention was focused on the SDW magnetism of thin Cr films because of its mediating role in exchange-coupled superlattices. For overviews of this field we refer the reader to reviews which have been published in recent years [15–17]. In particular, it has been shown theoretically [18, 19] and experimentally [20–22] that thin Cr layers sandwiched between Fe layers undergo a transition from a commensurate AF state to an incommensurate SDW magnetic order with increasing Cr layer thickness. For a [100] oriented layer, a SDW is expected to first occur at a thickness of about 3 nm, corresponding to half of a SDW period of 20 monolayers (ML). Here one ML corresponds to a thickness of 0.144 nm, neglecting thermal expansion. The details of the SDW order depend, however, on the specific boundary conditions, in particular on the adjacent metal layer, the interface roughness and the Cr orientation [16]. Furthermore, due to finite-size scaling, the Néel temperature was found to depend on the film thickness [20, 22]. Recent Mössbauer experiments on Cr/V(100) superlattices by Almokhtar *et al* [23] have shown that Cr layers are non-magnetic at a thickness below 2 nm and at a temperature of 15 K. However, the Cr magnetism is restored for thicknesses larger than 3 nm. Mössbauer and neutron scattering experiments confirmed that there is a node of the SDW at the Cr/V interface as soon as the Cr layer thickness is large enough to support an SDW of Cr confined by V [23, 24]. Thus V/Cr and Fe/Cr behave quite differently as regards the magnetic state of Cr at low temperatures. In Fe/Cr(100), due to the ferromagnetic boundaries, Cr exhibits a layer-wise commensurate antiferromagnetic structure up to 20 ML and an incommensurate SDW for larger thicknesses with an antinode at the Fe/Cr interface. In V/Cr(100), in contrast, Cr is most probably non-magnetic below 20 ML and develops an incommensurate SDW state for larger thicknesses with a node at the V/Cr interface. Much less is known about the Cr(110) orientation. Neutron scattering experiments on (110) oriented Fe/Cr multilayers revealed, however, that the commensurate AF phase is the stable phase at 300 K, while at low temperatures a phase transition to the incommensurate SDW occurs [25, 26]. The magnetic phase diagram of V/Cr(110) is not known at the present time. However, it may be expected that for this orientation a node of the SDW develops for V thicknesses beyond 20 MLs similar to the case for the [100] orientation. From a theoretical point of view, a ML of Cr on V(001) is found to be ferromagnetically ordered with an enhanced moment compared to the bulk, inducing an antiparallel moment in V at the interface, similar to the situation for Fe/V [27, 28]. Thus the experimentally found node at the Cr/V interface may be an artefact, resulting from a compensation of Cr and V moments at the interface. All this requires more detailed investigation in the future.

Here we present a detailed determination of T_c as a function of the V and Cr thicknesses, giving special attention to the thickness range where we expect the onset of SDW order in Cr.

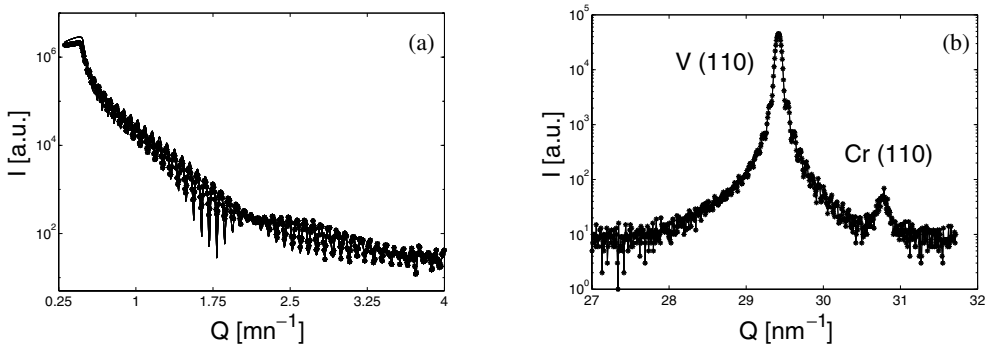

Figure 1. X-ray measurements of a typical Cr/V/Cr trilayer system. (a) Reflectivity measurement of a Cr/V/Cr trilayer and a fit with the Parratt formalism. (b) A Bragg scan of a Cr/V/Cr trilayer; the sapphire peak is shown reduced for clarity.

Interestingly we observe a strong suppression of the superconducting transition temperature for a Cr layer thickness for which we expect the onset of a SDW state. This suppression is not explained by the classical Werthamer theory for SC/NM proximity effects [1]. Furthermore, unlike in the FM/SC proximity effect, where a re-entrant behaviour of superconductivity can be observed with increasing FM film thickness [5], the superconductivity remains suppressed in the case of V/Cr(100) for Cr layer thicknesses beyond 8 nm.

2. Preparation and experimental details

We have prepared Cr/V/Cr trilayers by rf sputtering on high-quality Al_2O_3 $(11\bar{2}0)$ substrates at $T_{sub} = 593$ K. The base pressure of the system was 5×10^{-8} mbar before sputtering and we used 99.99% pure Ar at a pressure of 5×10^{-3} mbar as the sputter gas. The growth rate was 0.04 nm s^{-1} for Cr and 0.03 nm s^{-1} for V. After deposition, the films were covered by a 2 nm thick Al_2O_3 cap layer to avoid uncontrolled oxidation. *Ex situ* out-of-plane x-ray Bragg reflection measurements (see figure 1(b)) revealed a (110) texture of V and Cr.

In order to reliably determine T_c as a function of layer thickness (d_V or d_{Cr}), it is essential to ensure identical conditions during sample preparation and to provide control over the relative layer thicknesses with an accuracy as high as possible. Therefore a series of ten samples were prepared within each deposition run. To obtain a constant layer thickness, the ten substrates of each series were placed in a circle on the substrate holder and the substrate holder was positioned at the symmetric position of the cylindrically shaped discharge. For the preparation of the layers with the variable thickness, the substrate holder was placed with its centre at the edge of the discharge, thus using the natural gradient of the deposition rate. The gradient has been determined accurately by using calibration samples and covered a thickness range of about a factor of 6.

Following this procedure, we prepared three different series of samples. In series I (see table 1) we kept the Cr thickness of $d_{Cr} = 10$ nm constant and varied the V thickness in the range $d_V = 20.6$–120 nm. Two further series with variable d_{Cr} and constant $d_V = 30$ nm were prepared. In series II, d_{Cr} ranged from 1.1 to 4.1 nm; series III covered the thickness range of d_{Cr} from 4.1 to 15.5 nm. For calibration purposes (see below) we prepared one extra series (series 'Cal' in table 1) of ten pure V films in the thickness range $d_V = 5$–30 nm using the same preparation conditions as mentioned above.

By means of *ex situ* x-ray reflectivity measurements (see figure 1(a)) the layer thicknesses were determined from fits to model reflectivities according to the Parratt formalism [29]. For

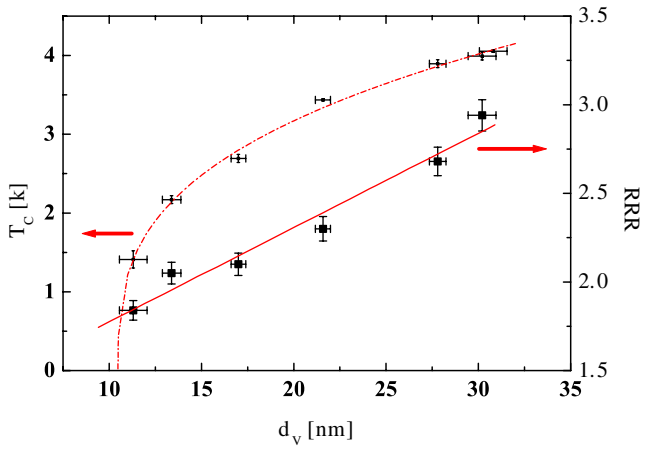

Figure 2. RRR and superconducting transition temperature T_c plotted against the vanadium layer thickness d_V for a series of single vanadium layers without adjacent Cr layers. The dashed curve shows an exponential fit to the T_c-data (for series 'Cal' from table 1).

the bottom and top Cr layers we obtained identical thickness within measurement accuracy. The interface roughness was found to be typically below $\sigma \sim 1$ nm. Thin-film oscillations (Kiessing fringes) are discernible up to a scattering vector $Q > 5$ nm^{-1}, indicating an overall high interface quality. Cr and V are chemically very similar and tend to interdiffuse easily. Modelling the electron density profile of the layer structure again with the Parratt formalism, we found no significant indication of interdiffusion.

The superconducting transition temperature T_c was measured by means of dc resistivity measurements, using a standard four-probe technique with silver-painted contacts. The resistivity measurements were made down to 1.3 K. If necessary, i.e. in the case of a transition temperature below 1.3 K, an ac susceptibility set-up in a He^3 cryostat for temperatures down to 0.3 K was employed. The ac susceptibility was measured by a mutual inductance technique at a frequency of 72 Hz and an amplitude of the ac field of 1 Oe (rms). The film plane was oriented perpendicular to the magnetic field.

3. The superconducting transition of single V layers

In V metals, T_c depends sensitively on the electron mean free path. For pure V bulk single crystals, $T_c = 5.3$ K, whereas for thin films, one usually has a smaller electron mean free path and T_c is notably lowered. The effect is caused by lifetime broadening of states at the Fermi level. Figure 2 represents our results obtained for single V films of different thicknesses and without Cr boundary layers. For these samples we find that T_c decreases continuously with decreasing film thickness and decreasing residual resistivity ratio (RRR), defined as

$$\mathrm{RRR} = \frac{R(295\,\mathrm{K})}{R(5\,\mathrm{K})} \doteq \frac{\rho(295\,\mathrm{K})}{\rho(5\,\mathrm{K})}. \tag{1}$$

Below a critical film thickness of $d_V^{crit} = 10.5$ nm, corresponding to RRR $\cong$ 1.7, the V film is not superconducting. The decrease of T_c is mainly caused by the reduced electron mean free path and is not due to finite-size scaling. Therefore we have fitted the experimental points to an exponential expression, which serves as a guide to the eye.

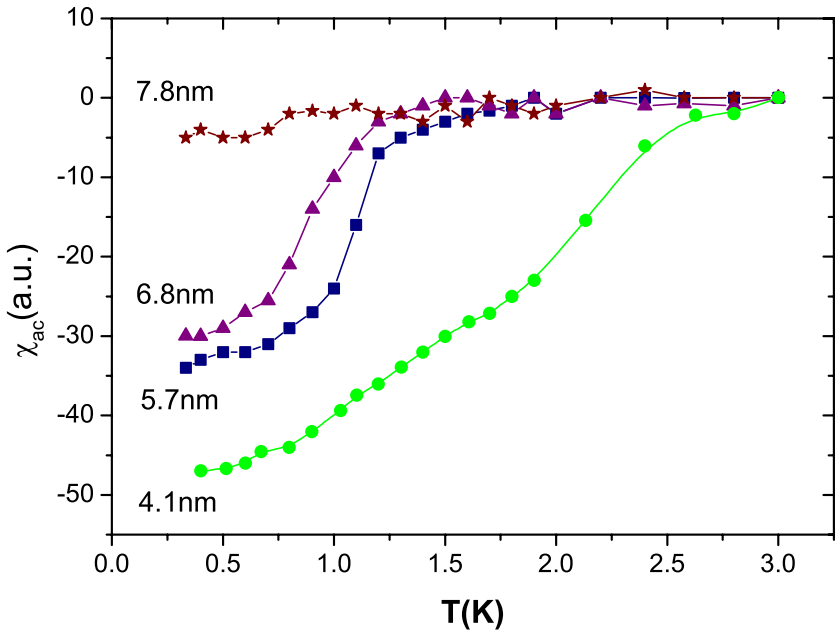

Figure 3. The ac susceptibility of Cr/V/Cr trilayers with the magnetic field applied perpendicular to the film plane is plotted versus temperature. Each curve refers to one specific d_{Cr} given in the figure and a constant $d_V = 30$ nm (for samples of series III in table 1).

Table 1. RRR and measured layer thicknesses for the sample series.

Series	d_{Cr} (nm)	d_V (nm)	RRR
I	10	20.6–120	1.6–4.4
II	1.1–4.1	30	3.3 (average)
III	4.1–15.5	30	3.3 (average)
Cal	N.A.	5–30	1.7–3.1

4. The superconducting transition of Cr/V/Cr trilayers

In figures 3 and 4 we show representative examples of ac susceptibility and resistivity measurements, respectively, for samples from table 1. In the resistivity curves we observe a two-step transition indicating a slight macroscopic inhomogeneity with a total transition with a width ΔT of about 0.2 K. The superconducting transition temperature T_c is defined as the mid-point of the transition. In the ac susceptibility one notes a broad transition with a susceptibility amplitude increasing down to the lowest temperatures. This is due to the orientation of the ac field perpendicular to the film plane, causing a divergence of the internal magnetic field of the superconducting film in the Meissner phase. Thus vortices enter the film below T_c and during one field cycle penetrate the film from the edges up to the ac penetration depth. The ac penetration depth decreases with the temperature below T_c, giving rise to the temperature dependence of the susceptibility amplitude observed in figure 3. The transition temperature T_c determined from the onset of the ac susceptibility coincides with T_c determined from the resistivity curves.

The residual resistivity $\rho(5\ \mathrm{K})$ allows a quantitative determination of the mobility of the conduction electrons. From our dc resistivity measurements we obtain the RRR as defined in

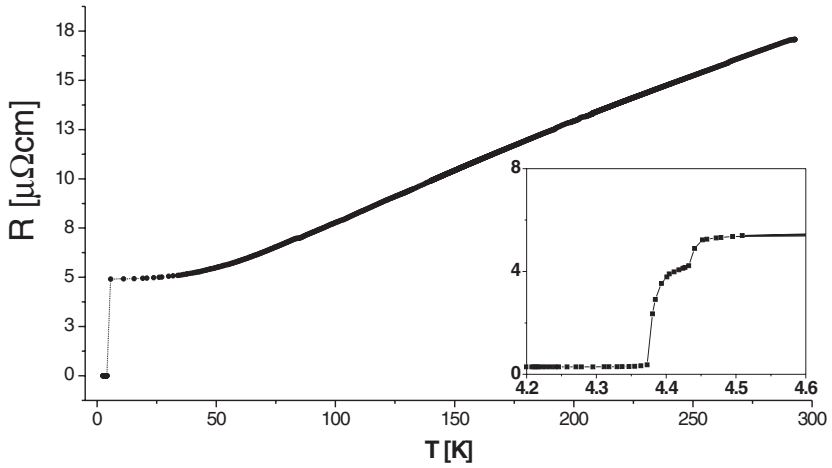

Figure 4. Resistivity versus temperature for a Cr/V/Cr trilayer. The inset shows detail of the superconducting transition on an enlarged scale. The vanadium thickness was 63 nm and the Cr thickness 10 nm.

(1) for each sample and get an average RRR for series II and III (see table 1). This gives an average of $\rho(5\ \mathrm{K}) = 5\ \mu\Omega$ cm for series II and III.

With $\rho(5\ \mathrm{K})$ we can calculate the electron mean free path l, using Pippard's equation [30]:

$$\langle v_{Fl} l \rangle = \left(\frac{\pi k_B}{e}\right)^2 \frac{\sigma_{el}(5\ \mathrm{K})}{\gamma}. \tag{2}$$

Here $\gamma = 9.26$ mJ mol^{-1} K^{-2} is the electronic contribution to the specific heat, $v_{Fl} = 3 \times 10^7$ cm s^{-1} is the Fermi velocity for V and $\sigma_{el}(5\ \mathrm{K}) = (\rho(5\ \mathrm{K}))^{-1}$. From this we obtain $l = 5.3$ nm for sample series I and II.

In figure 5 we show how the superconducting transition temperature depends on the V film thickness $T_c(d_\mathrm{V})$ for sandwiching between two Cr layers of constant thickness $d_\mathrm{Cr} = 10$ nm. The arrows indicate a T_c-value below the accessible temperature range of our experimental set-up.

Below a V layer thickness of $d_\mathrm{V} = 50$ nm one observes a strong decrease of the transition temperature. The fit to the measured data points indicates a critical thickness $d_\mathrm{V}^{crit} \cong 25$ nm of V below which the superconductivity vanishes. This increase of the critical thickness as compared to the single V layer ($d_\mathrm{V}^{crit} \cong 10$ nm; see section 3) is due to the effect of Cr on the superconductivity in the Cr/V/Cr trilayer system.

For a more detailed investigation of the influence of Cr on the superconductivity of V, the transition temperature was determined as a function of the Cr layer thickness $T_c(d_\mathrm{Cr})$ with d_V fixed at $d_\mathrm{V} = 30$ nm to provide a maximum sensitivity to variations in the Cr layer thickness. The Cr cap and bottom layer thicknesses were varied between $d_\mathrm{Cr} = 1.2$ and 15.5 nm. The results of dc resistivity measurements (series II, $d_\mathrm{Cr} = 1.1$–4.4 nm) and ac susceptibility measurements (series III, $d_\mathrm{Cr} = 4.1$–15.5 nm) are shown in 6. At $d_\mathrm{Cr} = 0$ nm we have inserted $T_c = 4.2$ K taken from the single V layer of corresponding thickness; the data above $d_\mathrm{Cr} = 8$ nm are omitted for clarity, since no superconducting transition could be identified. The arrow indicates the first experimental point with a T_c below the accessible temperature range.

We observe a smooth decrease of T_c with increasing Cr layer thickness which qualitatively follows the theoretically predicted [1, 31] and experimentally reported [32] AF/SC and NM/SC

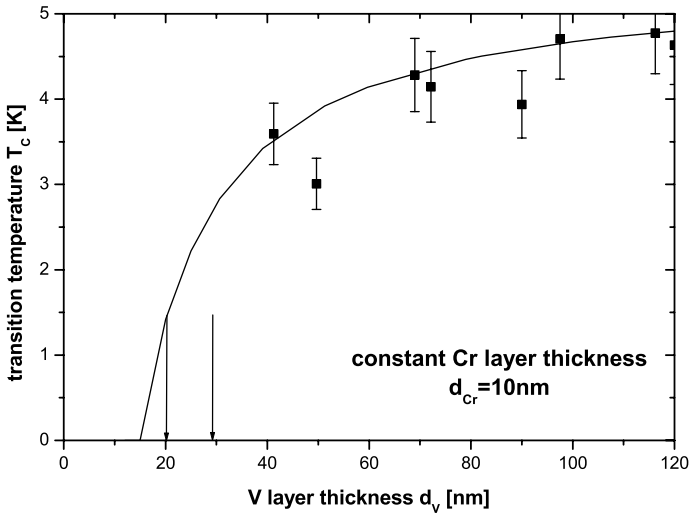

Figure 5. Superconducting transition temperature as a function of the V layer thickness in a V layer sandwiched between two Cr layers with fixed thicknesses $d_{\mathrm{Cr}} = 10$ nm. The solid curve represents a fit to the dGW theory (see the text). The arrows indicate data points with a T_c below the accessible temperature range.

proximity effects. A slight increase of T_c is noticed at about 4.5 nm, which is similar to the feature noticed previously by Davis *et al* [10] for V/Cr multilayers. We believe that in our case this is an experimental artefact, due to the fact that at 4.1 nm two different sample series have been joined together. Nevertheless, we will investigate this effect in more detail in the future. However, at $d_{\mathrm{Cr}} = 5$–7 nm we notice another steep decline of T_c until SC is completely suppressed for $d_{\mathrm{Cr}} \geqslant 8$ nm. Re-entrance of superconductivity at larger Cr layer thickness was not observed. For AF or NM layers the strong suppression of T_c is unexpected. Moreover, the coincidence of this feature in the $T_c(d_{\mathrm{Cr}})$ curve with the expected onset of an incommensurate SDW magnetism may indicate a connection between the $T_c(d_{\mathrm{Cr}})$ curve and the magnetic state of Cr.

5. Comparison with standard AF/SC theory

The theoretical approach to the AF/SC proximity effect is based on the assumption of a weak influence of the AF state on the superconductivity. Because of this the AF/SC proximity effect is usually treated as a NM/SC proximity effect. Following this assumption, we treat Cr as a non-magnetic metal as regards the theoretical description of the V/Cr proximity effect.

The classical theory describing the NM/SC proximity effect of finite layer thickness was developed by Werthamer [1], extending the theoretical work of de Gennes [31] beyond the '*Cooper limit*'. Within the '*dirty limit*' approximation a space-dependent variation of the Cooper-pair density n_S was introduced. This leads to a set of three equations (3), which when combined yield an implicit solution for the critical temperature T_c of the total system:

$$\ln\left(\frac{T_{c,S}}{T_c}\right) = \chi(\xi_S^2 k_S^2) \tag{3a}$$

$$\ln\left(\frac{T_{c,N}}{T_c}\right) = \chi(-\xi_N^2 k_N^2) \tag{3b}$$

$$\mathfrak{D}(\varepsilon_F)\xi_S^2 k_S \tan(k_S d_S) = \mathfrak{D}(\varepsilon_F)\xi_N^2 k_N \tanh(k_N d_N). \tag{3c}$$

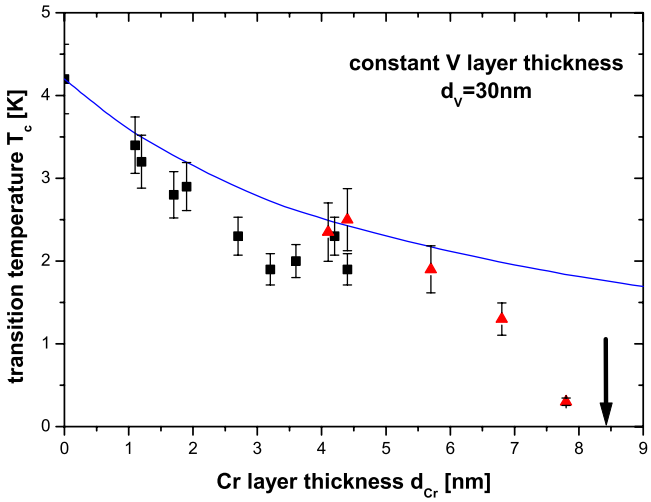

Figure 6. Superconducting transition temperature as a function of the Cr layer thickness. The V layer thickness is held constant ($d_{\mathrm{V}} = 30$ nm). Two sample series (series II: squares; series III: triangles) are joined together at the Cr thickness of 4.1 nm. The solid curve represents the fit to the dGW theory (see the text) and the arrow indicates the first data point with a T_c below the accessible temperature range.

Here $T_{c,S}$ is the critical temperature for the superconducting layer and $T_{c,N}$ is the critical temperature for the normal-conducting layer in contact with the superconducting layer. $k_{S,N}$ are free parameters, $\mathfrak{D}(\varepsilon_F)$ is the electron density of states at the Fermi level and χ is given by the relation

$$\chi(z) = \Psi(\tfrac{1}{2} + \tfrac{1}{2}z) - \Psi(\tfrac{1}{2}),$$

where Ψ is the digamma function and ξ is an effective coherence length of a system of finite thickness, which follows from the BCS coherence length $\xi_0 = 2\hbar v_F/\pi E_g$ on properly weighting according to the mean free path l:

$$\xi = \sqrt{\frac{\xi_0 l}{3.4}} = \left(\frac{\pi\hbar k_B}{6e^2}\frac{\sigma}{\gamma}\frac{1}{T_c^0}\right)^{-1}. \tag{4}$$

The function $\chi(z)$ can be approximated for $z \ll 1$ [1, 32] by

$$\chi(z) \cong \begin{cases} \ln\left[1 + \dfrac{\pi^2}{4}z\right], & \text{for } z \geqslant 0 \\ \dfrac{\pi^2}{4}\ln[1+z], & \text{for } z \leqslant 0 \end{cases} \tag{5}$$

which enables us to eliminate the free parameters $k_{S,N}$ and to write just one equation describing the thickness dependence of T_c:

$$\sqrt{\left(\frac{T_{c,S}}{T_c} - 1\right)}\tan\left[\frac{2d_S}{\pi\xi}\sqrt{\frac{T_{c,S}}{T_c} - 1}\right] = \frac{\mathfrak{D}_N(\varepsilon_F)}{\mathfrak{D}_S(\varepsilon_F)}\frac{\pi}{2}\tanh\left[\frac{d_N}{\xi}\right]. \tag{6}$$

Using equation (6), the solid lines for $T_c(d_{\mathrm{Cr}})$ and $T_c(d_{\mathrm{V}})$ as shown in figures 5 and 6 were calculated.

The experimental parameters used for the solution of equation (6) are the thicknesses d_{Cr} and d_{V}, the coherence length ξ, as determined from the electron mean free path, and the value $T_c = 4.2$ K for a single V layer taken from figure 2.

We notice that the theory is able to explain the overall shape of the measured data in figure 5. However, there is a deviation as regards the experimentally observed and theoretically predicted critical thickness. The theoretical curve in figure 6 is also in fair agreement with the experimental data up to a Cr thickness of $d_{\mathrm{Cr}} \approx 6$ nm. We also notice a shallow maximum at 4.5 nm, which might be an experimental artefact due to joining two sample series at this point. In addition, an offset is noticed, with the measured T_c being systematically lower than the theoretical curve. The systematic deviation can be attributed to some inelastic scattering in the interface region or in the interior of the Cr layers. However, in figure 6 there is one feature which clearly cannot be explained by the classical theory of the proximity effect. This is the structure of the $T_c(d_{\mathrm{Cr}})$ curve for a larger Cr thickness with the rapid quenching of superconductivity for $d_{\mathrm{Cr}} \geqslant 6$ nm. This thickness range correlates with the expected onset of the incommensurate SDW in Cr, suggesting that the incommensurate SDW order may be responsible for the rapid quenching.

6. Summary and conclusions

We have studied the AF/SC proximity effect by studying the dependence of the critical temperature in Cr/V/Cr trilayers as a function of the V thickness with fixed Cr thickness and as a function of the Cr thickness with fixed V thickness. In the latter case we find that T_c decreases smoothly, consistently with the classical Werthamer theory, until $d_{\mathrm{Cr}} \approx 6$ nm. A slight systematic deviation of the experimental points and the theoretical curve in this region can be explained by assuming some additional pair-breaking scattering in the Cr layer or at the interfaces [10]. However, beyond $d_{\mathrm{Cr}} = 6$ nm we find a dramatic change in the behaviour of $T_s(d_{\mathrm{Cr}})$. The superconducting transition temperature drops faster than expected with increasing Cr thickness until the superconductivity vanishes completely. This finding clearly does not fit into the classical theoretical description. The steep drop of the transition temperature coincides with the thickness for which an onset of an incommensurate SDW state in thin Cr films should be expected and has been observed for the [100] orientation [23], thus suggesting an intricate correlation between the magnetic transition in Cr and the drop in $T_c(d_{\mathrm{Cr}})$. Recent Mössbauer and neutron scattering investigations of V/Cr superlattices reported an SDW state with a node at the V/Cr interface [23, 24], implying a strong suppression of the Cr magnetic moments at the Cr/V interface. It is puzzling that a node of the SDW at the V/Cr interface can quench the superconductivity. On the other hand, theory predicts an enhanced moment for a ML of Cr on V(001) with an antiparallel induced moment of V at the interface [27, 28], which contradicts the notion of a node at the interface. At the present time we cannot offer a conclusive explanation for the observations and we can only speculate about their origin here. First, it seems possible that the interface magnetism of the first few (mixed) Cr/V ML changes with the onset of an SDW state. Second, a change of the electronic band structure accompanying the magnetic transition in Cr may cause the drop in $T_c(d_{\mathrm{Cr}})$. According to the theory of the proximity effect, the quantum mechanical transparency is one important parameter determining quantitatively the suppression of T_c [6, 33]. In our present case of the Cr/V interface, a higher value for the transparency in the SDW state compared to the non-magnetic state thus could in principle cause a drop in $T_c(d_{\mathrm{Cr}})$.

Acknowledgments

This work was supported by 'Sonderforschungsbereich' (SFB) 491 of the 'Deutsche Forschungsgemeinschaft' (DFG). The authors thank Dr K Hirai for valuable discussions and gratefully acknowledge J Podschwadek and S Erdt-Böhm for technical help during sample preparation.

References

[1] Werthamer N R 1963 *Phys. Rev.* **132** 2440
[2] Wong H K, Jin B Y, Yang H Q, Ketterson J B and Hilliard J E 1986 *J. Low Temp. Phys.* **63** 307
[3] Jiang J S, Davidovic D, Reich D H and Chien C L 1995 *Phys. Rev. Lett.* **74** 314
[4] Lazar L, Westerholt K, Zabel H, Tagirov L R, Goryunov Yu V, Garif'yanov N N and Garifullin I A 2000 *Phys. Rev.* B **61** 3711
[5] Garifullin I A, Tikhonov D A, Garif'yanov N N, Lazar L, Goryunov Yu V, Khlebnikov S Ya, Tagirov L R, Westerholt K and Zabel H 2002 *Phys. Rev.* B **66**
[6] Tagirov L R 1988 *Physica* C **307** 145
[7] Garifullin I 2002 *J. Magn. Magn. Mater.* **240** 571
[8] Hauser J J, Theuerer H C and Werthamer N R 1966 *Phys. Rev.* **142** 118
[9] Cheng Y and Stearns M 1990 *J. Appl. Phys.* **67** 5038
[10] Davis B, Zheng J Q, Auvil P R, Ketterson J K and Hilliard J E 1988 *Superlatt. Microstruct.* **4** 465
[11] Fawcett E 1988 *Rev. Mod. Phys.* **60** 209
[12] Overhauser A W 1962 *Phys. Rev.* **128** 1437
[13] Corliss L, Hastings J and Weiss R 1959 *Phys. Rev. Lett.* **3** 211
[14] Bykov V *et al* 1958 *Dokl. Akad. Nauk* **4** 1149
[15] Pierce D T, Unguris J, Celotta R J and Stiles M D 1999 *J. Magn. Magn. Mater.* **200** 290
[16] Zabel H 1999 *J. Phys.: Condens. Matter* **11** 9303
[17] Fishman R S 2001 *J. Phys.: Condens. Matter* **13** R235
[18] Hirai K 1999 *Phys. Rev.* B **59** R6612
[19] Fishman R S and Shi Zhu-Pei 1999 *Phys. Rev.* B **59** 13 849
[20] Fullerton E E, Bader S D and Robertson J L 1996 *Phys. Rev. Lett.* **77** 1382
[21] Schreyer A, Majkrzak C F, Zeidler Th, Schmitte T, Bödeker P, Theis-Bröhl K, Abromeit A, Dura J and Watanabe T 1997 *Phys. Rev. Lett.* **79** 4914
[22] Schmitte T, Schreyer A, Leiner A, Siebrecht R, Theis-Bröhl K and Zabel H 1999 *Europhys. Lett.* **48** 692
[23] Almokhtar M, Mibu K, Nakanishi A, Kobayashi T and Shinjo T 2000 *J. Phys.: Condens. Matter* **12** 9247
[24] Mibu K and Shinjo T 2002 *ICMFS 2002: 17th Int. Coll. on Magnetic Films and Surfaces (Kyoto, Japan) (digest)* p 356
Mibu K and Shinjo T 2002 *J. Phys. D: Appl. Phys.* at press
[25] Fritzsche H, Hauschild J, Nawrath T, Hoser A, Welzel S, Graf H A and Maletta H 2000 *Physica* B **276** 590
[26] Fritzsche H, Bonn S, Hauschild J, Klenke J, Prokes K and McIntyre G J 2002 *Phys. Rev.* B **65**
[27] Boussendel A and Haroun A 1998 *Thin Solid Films* **325** 201
[28] Hamad B A and Khalifeh J M 2001 *Surf. Sci.* **492** 161
[29] Parratt L G 1954 *Phys. Rev.* **59** 359
[30] Pippard A 1960 *Rep. Prog. Phys.* **23** 176
[31] de Gennes P and Sarma G 1963 *J. Appl. Phys.* **34** 1380
[32] Jin B and Ketterson J 1989 *Adv. Phys.* **38** 189
[33] Radovic Z, Dobrosavljevic-Gruji L, Buzdin A I and Clem J R 1988 *Phys. Rev.* B **38** 2388